

Resistance Spot Welds of 304L Austenitic Stainless Steel, Part 3 : 1 & 1, 1 & 2 and 2 & 2 mm Thickness of Weld Joints

Nachimani Charde

Department of Mechanical Engineering, Faculty of Engineering, University of Malaya, 50603 Kuala Lumpur, Malaysia.

Email: nachicharde@yahoo.com

ABSTRACT

Part 1 of this research introduces the spot weld growth on 304L stainless steel, mainly by explaining information: such as the specimen size, static resistance, welding lobe, welding schedule, simulation, tensile shear load, failure mode, and elongation. In part 2, the analysis explains the dynamic resistance, force profile, electrically generated forging force, macro and micro structural orientation and also the hardness distribution. In part 3, the investigation reveals similar and dissimilar thicknesses: pertaining to macrograph orientation, electrode indentation and the weld growth. Three types of different thicknesses are investigated for the macrograph development and subsequently found the symmetrical weld bead geometry despite thicknesses. Electric current increment is mainly analysed in this experiments as it increases the weld size significantly. Strength tests show that the weld geometries have been widened in proportion to the escalation of electric currents. The astonishing factor is that the bead thickness reduction due to electrode indentation does not affect the tensile strengths at all.

Keywords: Spot welding, Stainless steel, Dissimilar thickness, Macrographs, Dissimilar hardness

1.0 INTRODUCTION

Joining the similar and dissimilar thicknesses of a common material becomes regular practise in resistance spot welding field. By joining the equal thickness materials, the weld beads are believed to be symmetrical whereas the unequal thicknesses have produced asymmetrical weld geometry. As to challenge this empirical view, the investigation has been conducted on 304L stainless steel coupons; having thicknesses of 1 and 2 mm. The pairs of welded joints cover 1 mm thickness separately [1, 2, 3], 2 mm thickness separately and both thickness joined together. What would be the outcome of macrograph views are the primary interest of this research. As such, the welded regions are scanned for macro structural view and finally unleash some useful information about the

indentation apart from the nuggets sizes [4, 5]. Fusion equilibrium manipulates the heat diffusion predominantly so there are no asymmetrical weld beads but only with the line of intersection that connects both sides [6, 7].

2.0 EXPERIMENTATION

The test samples are prepared in rectangular shape (200 mm x 25 mm x 1&2 mm) as shown in **Fig. 1** and its chemical and mechanical properties are tabulated in **Table 1**. A pair of water cooled copper electrode caps with truncated tips (diameters of 5 mm) is used to join these stainless steel coupons. Heat was calculated from the Joule's law as it is governed by, $Q=I^2Rt$; where R is the total resistance of base metals, I is the welding current and t is the welding time.

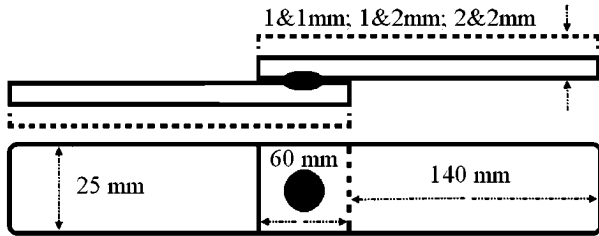


Figure 1: Lap joint of stainless steel coupon

Table 1: Chemical and mechanical properties

Element	1mm Weight %	2mm Weight %
C	0.03	0.03
Cr	18.12	18.14
Ni	8.11	8.13
Mn	1.166	1.205
Si	0.501	0.506
S	0.006	0.004
N	0.053	0.051
P	0.030	0.030
Hardness	81.7 (HRB)	86.2 (HRB)

The base metals are initially placed on the top of lower electrode of the spot welder (75kVA); as overlaying 60 mm on each other and then the initiating pedal is pressed. The welding process has started right after with squeezing process and; once the electrodes are well compressed the welding current is released then. Thereafter the electrode pressing mechanism (pneumatic based) consumes some time for solidification and returns to the home position of upper electrode. The basic process controlling parameters (the current and weld time) are set before the welding process starts with constant electrode pressing force (3kN) that supported by two round electrode tips. By varying the welding current and weld time from lower to higher values or thus, from poor welds to good welds and also beyond good welds, three sets of welding lobe curves are obtained for equal and unequal base metals.

Fig. 2, 3 and 4 show the welding lobe curves for 1&1 mm, 1&2 mm, and 2&2 mm sample thicknesses, respectively.

Acceptable weld regions are enclosed with continuous line to show the working windows. The multiple colors represent the quality of welded areas. Thus, the green color boxes that encapsulated with black color represent moderate good welds; the full green color boxes represent very good welds; the red color boxes that encapsulated with green color represent light expulsion welds; the red color boxes represent heavy expulsion welds and the black color boxes represent poor welds joints. Based on the welding lobe limits, a weld schedule (Table 2) is developed to cover from poor to expulsion cases. So the combinations of the nine (9) welding conditions are developed for the current and weld time as shown in Table 2.

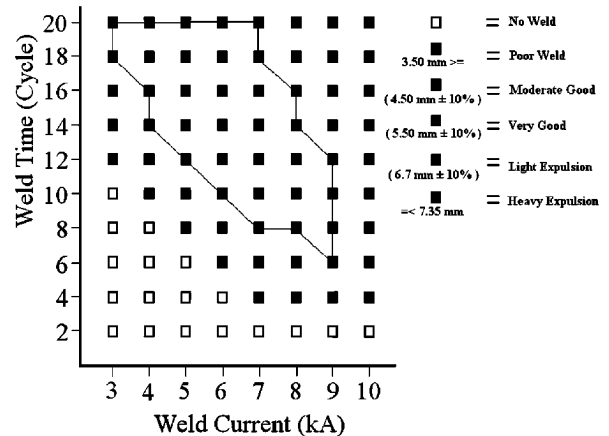


Fig. 2 : Welding lobe diagram of stainless steel for 1&1 mm

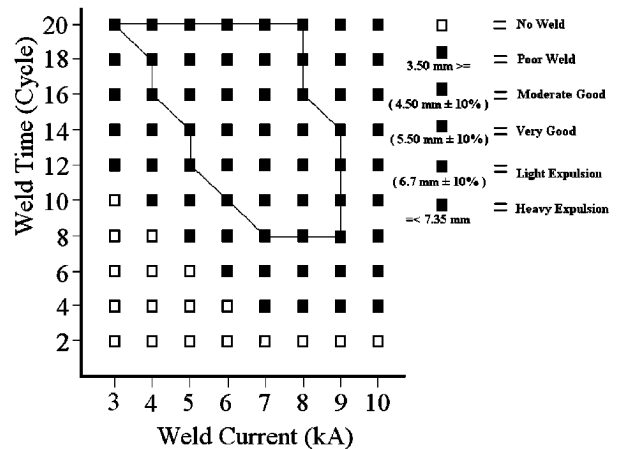


Fig. 3 : Welding lobe diagram of stainless steel for 1&2 mm

Table 2 : Weld schedule

Sample No.	Weld Schedule	Thickness (mm)	Electrode Tip Diameter (mm)	Force (kN)	Time (Cycle)	Current (kA)
1-7	1	1&1, 1&2, 2&2	5	3	10	6
8-14	2	1&1, 1&2, 2&2	5	3	10	7
15-21	3	1&1, 1&2, 2&2	5	3	10	8
22-28	4	1&1, 1&2, 2&2	5	3	15	6
29-35	5	1&1, 1&2, 2&2	5	3	15	7
36-42	6	1&1, 1&2, 2&2	5	3	15	8
43-49	7	1&1, 1&2, 2&2	5	3	20	6
50-56	8	1&1, 1&2, 2&2	5	3	20	7
57-63	9	1&1, 1&2, 2&2	5	3	20	8

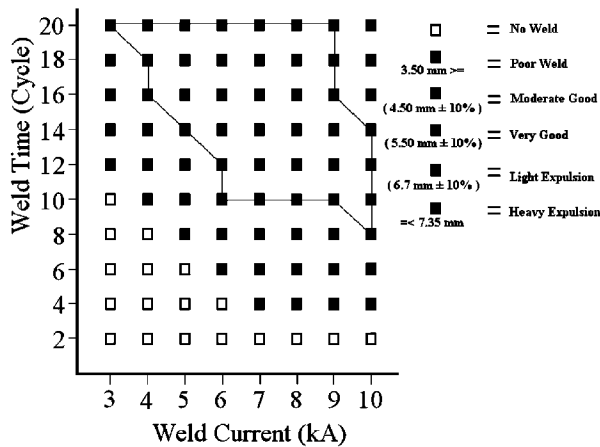


Fig. 4 : Welding lobe diagram of stainless steel for 2&2 mm

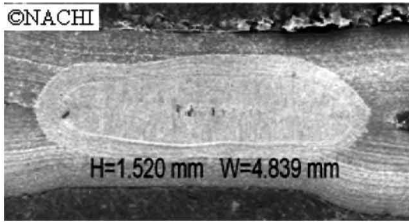
Every welding set up is identically followed as to produce welds without anomalies. Seven welded pairs are generated for each welding condition. The first five pairs of samples are used for tensile test-averaging, while the sixth sample is used for hardness measurement. The last one is cut across the line of its diameter and mounted using resin powder via hot press mount. The mounted samples are roughly polished using silicon papers 1200/800p and 600/200p and also continuously further polished using Metadi polishing cloth with suspension liquid of 0.05 micron. This polishing process has been conducted about thirty minutes to one hour on each sample until the shining surface is revealed. At last the ferric chloride

(500ml) is used to soak these well prepared (shining surface) samples in a pot about 30–45 minutes. After that the samples are rinsed off using plain water, dried up using air blower, applied anti-corrosion liquid, and kept in vacuum chamber for SEM analysis.

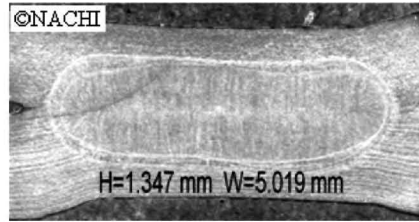
3.0 RESULTS AND DISCUSSION

3.1 Diameter of Weld Nuggets

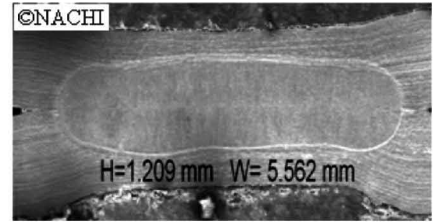
Having considered the macrograph for current increment (Fig. 5, 6 and 7), three noticeable regions are coexisted around the vicinity of spot welds [8]. Firstly the fusion zone (FZ) underwent complete melting process during heat generation and solidified once the electric current flow is over. It appeared to be coarser grains as the heat diffused horizontally in all direction. Compressing the molten zone have yielded indentation onto; and printed the corresponding mark over the fusion zones. The heat affected zone (HAZ) is coexisted due to the omni-directional heat diffusion. This led to the slight alteration of phases when complete solidification happened at fusion zone. It has been altered slightly from finer grains as compare to fusion zone. It started from the outer border of fused area and spread outwards in all direction to certain extends. The infused portion is not affected by any mean as the microstructures remain unchanged. Fig. 8 shows the width (diameter) against height (indentation) that obtained for current increments in this experiment [9].



(a) 6kA

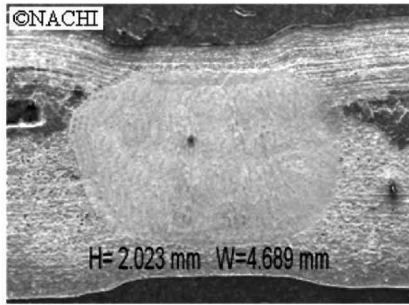


(b) 7kA

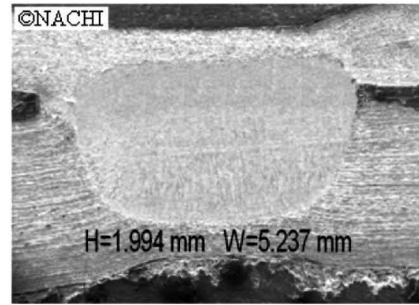


(c) 8kA

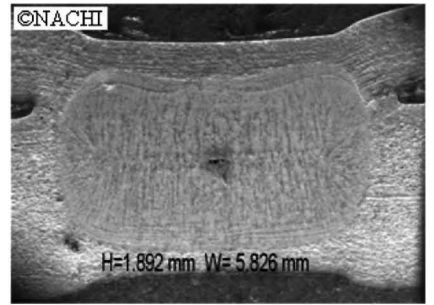
Fig. 5 : Macrograph of ASS (1&1 mm)



(a) 6kA

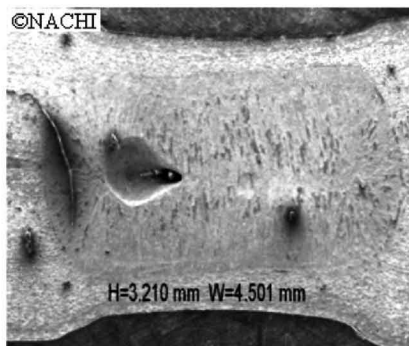


(b) 7kA

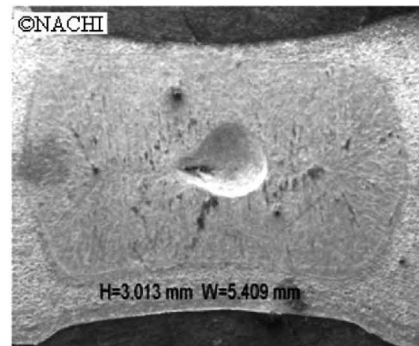


(c) 8kA

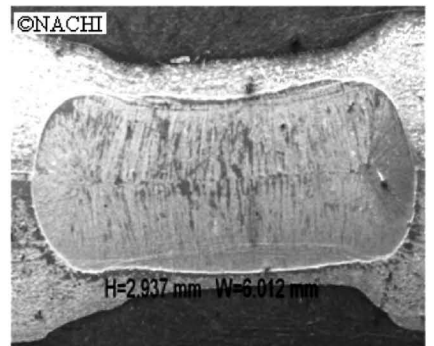
Fig. 6 : Macrograph of ASS (1&2 mm)



(a) 6kA



(b) 7kA



(c) 8kA

Fig. 7 : Macrograph of ASS (2&2 mm)

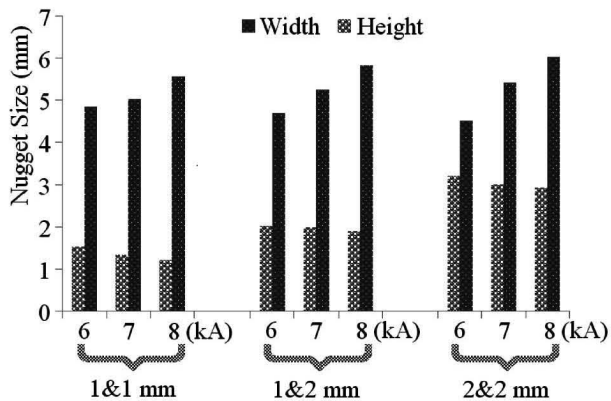


Fig. 8 : Nugget size of all the thickness

When the electric current is increased from 6 to 7 and 7 to 8 kA, the widths (diameter) have increased relatively and the associated heights are decreased respectively. These phenomena are recorded for all the thicknesses of base metals. However, in the 2&2 mm coupons, they have higher thicknesses and therefore the indentations deemed to be slightly higher than the 1&1 mm and 1&2 mm pairs. Unfortunately, when higher the electric current is forced to flow, than easier the porous existence within the fusion zones due to force inconsistencies.

3.2 Tensile Shear Test

The tensile test is conducted by employing 100 kN tensile

testing machine. The ultimate tensile strength is taken from the final value of loading forces at which the fracture begins. Five samples are developed to average the weld strength, in relation to a weld schedule. When the electric current is increased from 6 to 7 and 7 to 8 kA, more heat is developed across the weld areas and resulted diameter increments regardless of thicknesses. So the nugget diameters' increments have caused strong bonding between base metals and also require higher tensile force to break these joints. Similar incremental patterns are noticed when the weld time is increased from 10 to 15 and 15 to 20 cycles. **Fig. 9** compares the tensile strength of all, having the thickness of 1&1 mm, 1&2 mm and 2&2 mm weld joints. Although the strength incremental pattern seemed to be almost same for all the samples, the required breaking strength varies in real. The pair 2&2 mm thickness sheets require the pull-to-break force from 12.5 to 19.5 kN. The 1&2 mm mixed- thickness sheets require 7 to 9.5 kN while 1&1mm thickness sheets require 6.7 to 9 kN. Hence, it can be said that the tensile loading force is directly proportional to materials thickness in RSW [10, 11].

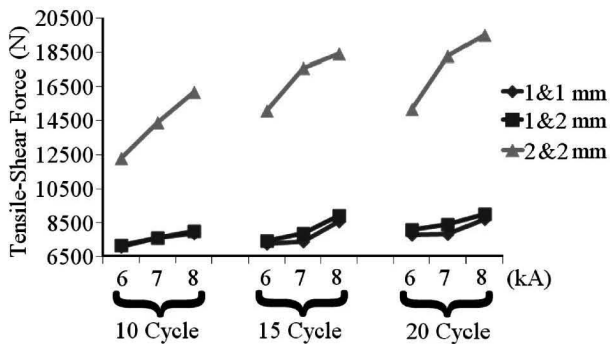


Fig. 9 : Tensile-shear test results

3.3 Hardness test results

The hardness test is carried out for all the thicknesses to understand the variations [12]. It is measured from left hand sides through the heat affected zones, then passing the fusion zones nucleus, again the other side of heat affected zones and ended on the right hand side of base metals [13]. The hardness of welded areas seemed to be noticeably increased but slightly varied from one thickness to another. Thus: when the 1 mm coupons are concerned over the welded areas, the hardness is escalated to 92 (HRB) from 81.5 (HRB). At the same time, the hardness of heat affected zones (HAZ) is increased to about 87 (HRB). **Fig. 10** shows the hardness distribution of all the weld joints. The unwelded areas (BM) of 2 mm thickness is measured to be an average hardness of 86 (HRB) but the welded areas seemed to be about 96 (HRB). Meanwhile the hardness of heat affected zones (HAZ) is lower than the fusion zones but higher than the base metals about 88 (HRB) as how the 1 mm thickness has yielded. Moreover the average hardness of dissimilar thickness welded zone is about 96 (HRB) approximately. The heat affected zones is resulted as an average of 89 (HRB) in the dissimilar weld joints. In overall the hardness of welded zones are slightly increased regardless of thicknesses due to the solidification process (**Fig. 10**).

4.0 CONCLUSION

This paper looks into the spot weld growth on 304L austenitic stainless steel with various thicknesses and; it concludes that

1. Increase in welding current within the welding lobe limits have resulted increment of weld nuggets width but simultaneously reduced the height of weld nuggets regardless of thicknesses.

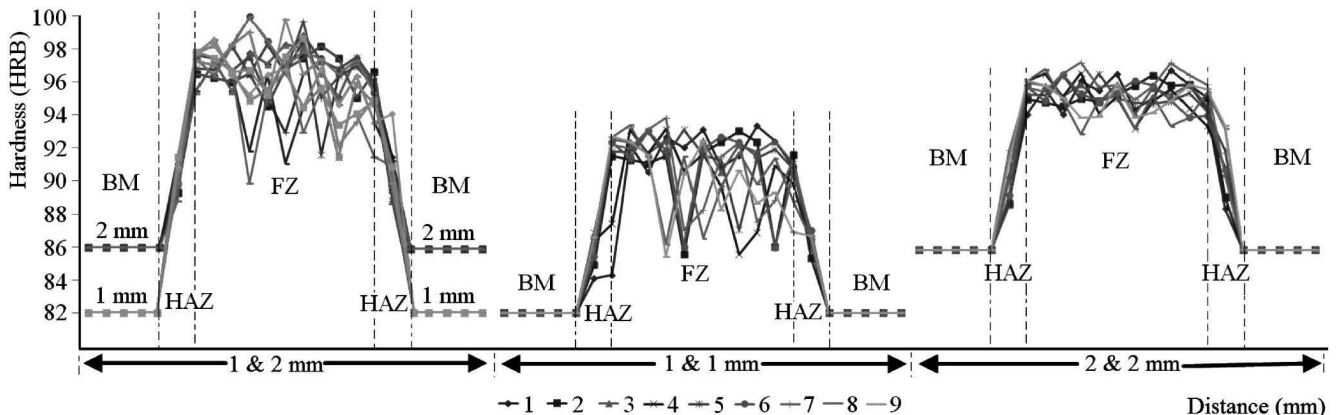


Fig. 10 : Hardness test results

2. The increments of tensile strength are observed due to the enlargement of welded areas within the welding lobe regions.
3. The simulation and experimental weld bead shapes are almost same to one another except the intersecting lines in the weld nuggets.
4. The hardness values of welded areas are slightly increased due to the solidification process. However the hardness distributions along the welded areas are produced fluctuations regardless of thicknesses. Unwillingly, the increase in welding current does not influence the changes in hardness distribution along the welded areas.

REFERENCES

- [1] Nachimani C, Resistance spot welds of 304L austenitic stainless steel, part 1: fundamental, simulation, weld growth, tensile strength and failure mode analysis, *Indian Welding Journal*, Vol 48, No.2, 2015.
- [2] Nachimani C, Resistance spot welds of austenitic stainless steel, part 2: signals measurement, dynamic resistance, electrically generated forging force, metallurgy and hardness distribution analysis, *Indian Welding Journal*, Vol 49, No.1, 2016.
- [3] Aravinthan A, Nachimani C, Analysis of spot welds growth on mild and stainless steel. *Welding Journal*, 143-147, 2011.
- [4] Aravinthan A, Nachimani C, Metallurgical study of spot welds growth on mild steel with 1mm and 2mm thicknesses. *Journal - The Institution of Engineers, Malaysia*, Vol. 72, No. 4: 46-54, 2011.
- [5] Dursun O, An effect of weld current and weld atmosphere on the resistance spot weld ability of 304L austenitic stainless steel. *Materials and Design*, Vol 29: 597-603, 2008.
- [6] Fukumoto S, Fujiwara K, Toji S, Yamamoto A, Small scale resistance spot welding of austenitic stainless steels. *Materials Science and Engineering A*, Vol 492: 243-249, 2008.
- [7] Jamasri MN, Ilman R, Soekrisno, Triyono, Corrosion fatigue behaviour of rsw dissimilar metal welds between carbon steel and austenitic stainless steel with different thickness. *Procedia Engineering*, Vol 10: 649-654, 2011.
- [8] Marashi P, Pouranvari M, Amirabdollahian S, Abedi A, Goodarzi M, Microstructure and failure behavior of dissimilar resistance spot welds between low carbon galvanized and austenitic stainless steels. *Materials Science and Engineering A*: 175-180, 2008.
- [9] Nachimani C, Spot weld growth on 304L austenitic stainless steel for equal and unequal thickness, *Caspian Journal of Applied Sciences Research*, 79-87, 2012.
- [10] Martín O, Tiedra PD, Lopez M, Juan MS, García C, Martín F, Blanco Y, Quality prediction of resistance spot welding joints of 304 austenitic stainless steel. *Materials and Design*, Vol 30: 68-77, 2009.
- [11] Pouranvari M, Effect of welding current on the mechanical response of resistance spot welds of unequal thickness steel sheets in tensile-shear loading condition. *International Journal of Multidisciplinary Sciences and Engineering*, Vol 2, No. 6: 178-189, 2011.
- [12] Shamsul JB, Hisyam M M, Study of spot welding of austenitic stainless steel type 304. *Journal of Applied Sciences Research*, Vol 3 (11): 1494-1499, 2007.
- [13] Yang Y, Qu X, Luo Y, Yang A, Effect of resistance spot welding parameters on the austenitic stainless steel 304 grade by using 23 factorial designs. *Advanced Materials Research*, Vol 216: 666-670, 2011.